



HAL
open science

Dispersion identification using the Fourier analysis of resonances in elastic and viscoelastic rods

Ramzi Othman, Gérard Gary, Robert H Blanc, Marie-Noëlle Bussac, Pierre Collet

► **To cite this version:**

Ramzi Othman, Gérard Gary, Robert H Blanc, Marie-Noëlle Bussac, Pierre Collet. Dispersion identification using the Fourier analysis of resonances in elastic and viscoelastic rods. International Conference on Acoustics Mechanics and the Related Topics of Mathematical Analysis, CNRS, Jun 2002, Frejus, France. pp.229-235, 10.1142/9789812704405_0034 . hal-01008078

HAL Id: hal-01008078

<https://hal.science/hal-01008078v1>

Submitted on 15 Mar 2024

HAL is a multi-disciplinary open access archive for the deposit and dissemination of scientific research documents, whether they are published or not. The documents may come from teaching and research institutions in France or abroad, or from public or private research centers.

L'archive ouverte pluridisciplinaire **HAL**, est destinée au dépôt et à la diffusion de documents scientifiques de niveau recherche, publiés ou non, émanant des établissements d'enseignement et de recherche français ou étrangers, des laboratoires publics ou privés.

DISPERSION IDENTIFICATION USING THE FOURIER ANALYSIS OF RESONANCES IN ELASTIC AND VISCOELASTIC RODS

R. OTHMAN AND G. GARY

*Laboratoire de Mécanique des Solides, Ecole Polytechnique, 91128, Palaiseau, France.
E-mail : othman@lms.polytechnique.fr*

R. H. BLANC

Trans Waves, 150 le Corbusier, 13008, Marseille, France.

M.N. BUSSAC AND P. COLLET

Centre de Physique Théorique, Ecole Polytechnique, 91128, Palaiseau, France.

A new method for identifying the dispersion relation in elastic and viscoelastic rods is presented. It relies on the multiple resonance of a strain measurement. The wave velocity is related to the resonance position whereas the damping is related to the resonance bandwidth. Applied to an aluminum bar, the method provides wave dispersion for frequencies up to 60 kHz.

1 Introduction

Wave dispersion in rods is due to geometric and (or) viscoelastic reasons. When the cross-section is circular the dispersion relation is governed by the Pochhammer-Chree equation^{4,5,12}, which was extended to viscoelastic rods by Zhao & Gary¹⁵. In the Split Hopkinson bar apparatus (SHB), experimental results are improved when wave dispersion is taken into account^{3,6-8}. Wave dispersion in rods is also used to investigate the viscoelastic properties of materials^{2,11}.

Dispersion may be experimentally determined by comparing the wave Fourier components measured at two points on the rod^{1,2,9}. Recently, Hillström & al.¹⁰ developed a multi-point method using least squares. In the present paper, a one-point method is developed using a spectral analysis of the resonant frequencies of the rod.

2 Theory

We consider a finite rod of length L (see Figure 1). ε denotes the longitudinal strain. A perturbation is generated at the left end of the rod. The right end of the bar is kept free from stress.

Henceforth, we assume that only the first longitudinal mode of propagation is excited⁵⁻⁷. In this case, the Fourier transform of the strain can be expressed by :

$$\tilde{\varepsilon}(a, \omega) = A(\omega)e^{-i\xi(\omega)a} + B(\omega)e^{i\xi(\omega)a}, \quad (1)$$

where

$$\xi(\omega) = k(\omega) + i\alpha(\omega) = \omega/c(\omega) + i\alpha(\omega) , \quad (2)$$

$\xi(\omega)$ is the complex wave number of the first mode of propagation and it takes account of geometric effects and (or) viscoelastic effects, $c(\omega)$ is the phase velocity and $\alpha(\omega)$ the attenuation.

The Fourier components of the strain at the left side (striker side, abscissa $-L$) of the bar are denoted by $\theta(\omega)$. Considering the boundary conditions, i.e. $\tilde{\varepsilon}(0, \omega) = 0$ and $\tilde{\varepsilon}(-L, \omega) = \theta(\omega)$, it follows that:

$$A(\omega) = -B(\omega) = \frac{\theta(\omega)}{e^{i\xi(\omega)L} - e^{-i\xi(\omega)L}} . \quad (3)$$

Introducing (3) into (1) enables the strain to be expressed as a function of the complex wave number and of the boundary conditions at the left side of the rod

$$\tilde{\varepsilon}(a, \omega) = \theta(\omega) \frac{e^{-i\xi(\omega)a} - e^{i\xi(\omega)a}}{e^{i\xi(\omega)L} - e^{-i\xi(\omega)L}} = -\theta(\omega) \frac{\sin(\xi(\omega)a)}{\sin(\xi(\omega)L)} . \quad (4)$$

In a first step, wave attenuation is neglected ($|\alpha(\omega)| \ll 1$). With low damping materials, this hypothesis is valid for most experimental applications. A correction must be made for high damping materials.

Denoting by $S(a, \omega)$ the strain spectrum, (4) and (5) yield :

$$S(a, \omega) = |\tilde{\varepsilon}(a, \omega)| = |\tilde{\theta}(\omega)| \left| \frac{\sin(k(\omega)a)}{\sin(k(\omega)L)} \right| . \quad (5)$$

The spectrum denominator becomes zero for the frequencies ω_n such that ^{13,14}:

$$k(\omega_n) = n\pi / L , \quad (6)$$

where n is a relative integer. For each n , unless the angular frequency ω_n nullifies the numerator as well as the denominator, a resonance occurs. The corresponding resonant frequencies are associated with the local maxima of the spectrum, so they are easily assessed. Therefore, when

$$\theta(\omega_n) \neq 0 \text{ and } \forall p \in \mathbb{N}, a/L \neq p/n , \quad (7)$$

the wave velocity is given by :

$$c(\omega_n) = \omega_n L / n\pi . \quad (8)$$

Henceforth, we reconsider (4). The numerator and the denominator are developed as follows :

$$\sin(\xi(\omega)x) = \sin(k(\omega)x)\cos(i\alpha(\omega)x) + \cos(k(\omega)x)\sin(i\alpha(\omega)x) . \quad (9)$$

We develop the sine and cosine to the second order of $\alpha(\omega)x$:

$$\cos(i\alpha(\omega)x) = 1 + \frac{\alpha^2(\omega)x^2}{2} + o(\alpha^2(\omega)x^2) , \quad (10a)$$

$$\sin(i\alpha(\omega)x) = i\alpha(\omega)x + o(\alpha^2(\omega)x^2) . \quad (10b)$$

Eqns. (5), (9) and (10) yield :

$$S^2(a, \omega) = |\theta(\omega)|^2 \frac{\alpha^2(\omega)a^2 + \sin^2(k(\omega)a)}{\alpha^2(\omega)L^2 + \sin^2(k(\omega)L)} . \quad (11)$$

We assume that ω is close to a resonance value ω_n . The attenuation is considered to be constant in this vicinity: $\alpha(\omega) = \alpha_n = \alpha(\omega_n)$. The sine is developed in the vicinity of ω_n :

$$\sin(k(\omega)x) = \sin(k(\omega_n)x) + x\mu_n \cos(k(\omega_n)x)(\omega - \omega_n) - \frac{1}{2}x^2\lambda_n \sin(k(\omega_n)x)(\omega - \omega_n)^2 + o((\omega - \omega_n)^2) , \quad (12)$$

$$\text{where } \mu_n = \left. \frac{\partial k}{\partial \omega} \right|_{\omega=\omega_n} \quad \text{and} \quad \lambda_n = \left. \frac{\partial^2 k}{\partial \omega^2} \right|_{\omega=\omega_n} .$$

Let $\delta\omega_n$ be half the bandwidth at the half-height. A development to the second order, with respect to $\delta\omega_n$, yields a simple expression for the wave damping coefficient:

$$\alpha_n^2 = \alpha^2(\omega_n) = \mu_n^2 \delta\omega_n^2 . \quad (13)$$

Since the waves attenuate as they advance, damping is negative^{13,14} :

$$\alpha_n = -\mu_n \delta\omega_n . \quad (14)$$

3 Experimental validation

3.1 Experimental set-up

A 3.019-m-long and 40-mm-diameter aluminium bar was considered. One strain gauge was cemented at $x = -1.567 \text{ m}$. Six tests were carried out. Three tests were carried out using a 15-cm-long aluminium striker having the same section as the bar and the other three tests were carried out using a 120-cm-long aluminium striker having also the same section as the bar. The striker velocity was about 16m/s. The measured strain in test 1 and its spectrum are shown in Figure 2. Signals were sampled with a frequency $f_s = 500 \text{ kHz}$. Fast Fourier Transforms (FFT) were performed using 10^6 -point long signals.

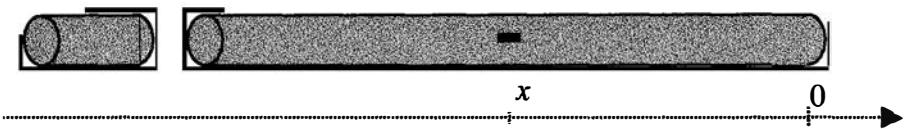


Figure 1. Simplified sketch of the experimental set-up.

3.2 Experimental results

For each test, the spectrum of the strain was computed using theFFT. Firstly, we determined the local maxima, which correspond to the resonant frequencies. Considering (6), the wave celerity is therefore assessed. Results of the five tests are superimposed in Fig.2. The observed sensitivity to the noise of the measurements is very small. The wave number was interpolated over the interval 0-60kHz as a polynomial function. Secondly, we determined the bandwidth of the resonance at the half-height of the peak. Knowing the derivative of the wave number with respect to the angular frequency, which was easily determined from the wave celerity, attenuation was calculated using (14). The values were also interpolated over the same interval as a polynomial function. Results for damping obtained from the five tests show a stronger sensitivity to noise than those obtained for wave celerity : they are more scattered.

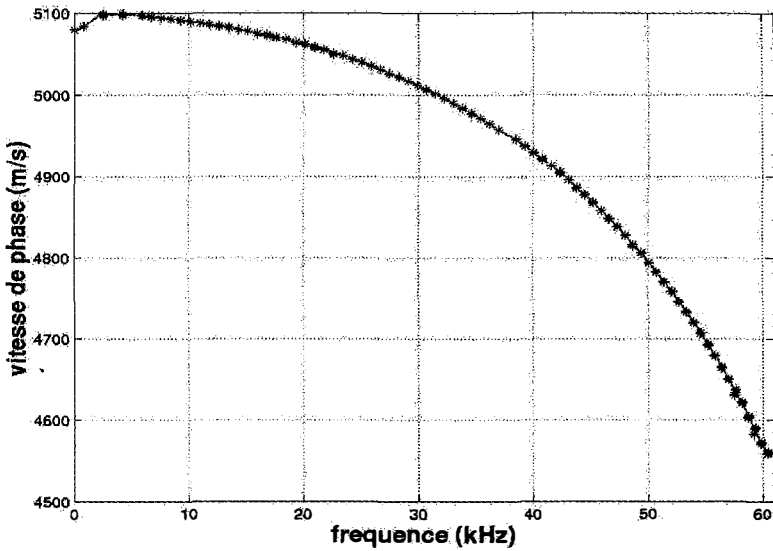


Figure 2. Longitudinal wave celerity

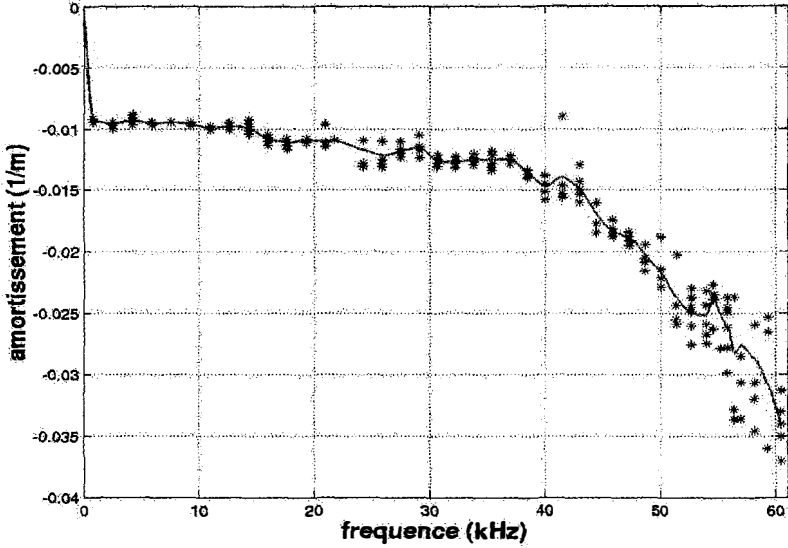


Figure 3. Longitudinal wave damping

3.3 Method precision

In this section, the quality of the dispersion relation determined in the above section is evaluated. The first incident wave of the measured strain (the first 0.06 ms, see Fig. 4) was extracted from the complete signal. The strain, after N round-trip in the bar, was then reconstructed, by transportation of the first incident wave, using the following equation :

$$\tilde{\varepsilon}^{(N)}(x, \omega) = \underbrace{\overbrace{\tilde{\varepsilon}_1^{(1)}(x, \omega)}^{\text{First incident wave}}}_{\text{Incident wave after } N \text{ round-trips}} \sum_{k=0}^{N-1} e^{-2i\xi(\omega)kL} - \underbrace{\overbrace{\tilde{\varepsilon}_1^{(1)}(x, \omega)}^{\text{First incident wave}}}_{\text{Re flected wave after } N \text{ round-trips}} \sum_{k=0}^{N-1} e^{-2i\xi(\omega)((k+1)L+x)}$$

This equation is easily derived by developing the fraction in (4). The measured and the rebuilt strains are then synchronised. The ascendant and descendant fronts start at the same time. The tail oscillations also appear as synchronised (Fig. 5). The phase difference between the two signals is very small. The wave celerity is therefore of a high accuracy. Damping is less accurate. The amplitude of the reconstructed strain is slightly greater than the amplitude of the measured one. However, the results are still satisfactory. The maximum relative error is less than 3.3% after the five wave round-trip in the bar (i.e. after 30 m shifting). This approach is then sufficient for classical SHPB applications where waves are shifted less than a length of the bar.

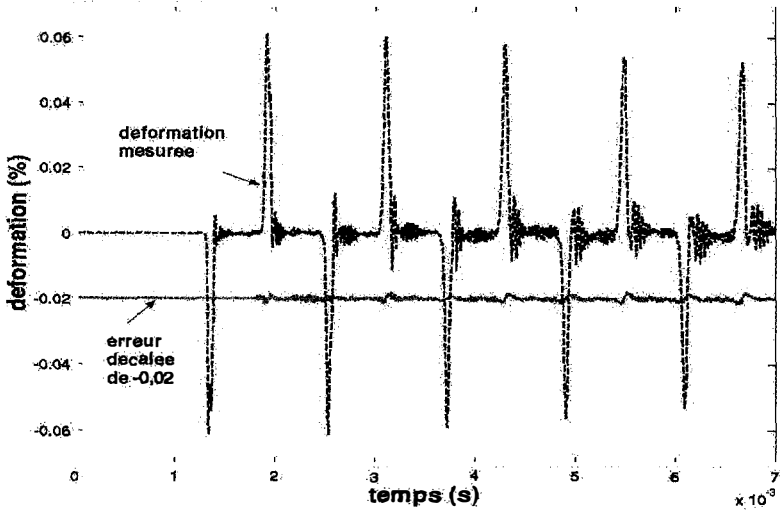


Figure 4. Method accuracy

4 Conclusion

A new method was presented to measure experimentally the longitudinal wave dispersion relation in finite elastic and viscoelastic rods. It is based on the spectral analysis of the measured strain at one point of the bar. We checked the validity of the method on an aluminium bar. The damping coefficient is slightly sensitive to noise, much more than the wave number. However, the method shows a high accuracy when waves are shifted by less than 30m.

References

1. Bacon, C. An experimental Method for Considering Dispersion and Attenuation in a Viscoelastic Hopkinson Bar. *Exper. Mech* **38** (1998) pp. 242-249.
2. Blanc, R. H. Détermination de l'équation de comportement des corps viscoélastiques linéaires par une méthode d'impulsion. *Symposium franco-polonais, Problèmes de Rhéologie*, Varsovie, IPPT Pan, W. Nowacki Ed., (1971) pp. 65-85.
3. Bussac, M. N., Collet, P., Gary, G. & Othman, R. An optimisation method for separating and rebuilding one-dimensional dispersive waves from multi-point measurements. Application to elastic or viscoelastic bars. *J. Mech. Phys. Solids* **50** (2002) pp. 321-349.

4. Chree, C. The equations of an isotropic elastic solid in polar and cylindrical co-ordinates, their solutions and applications. *Cambridge Phil. Soc. Trans.* **14** (1889) pp. 250-369.
5. Davies, R.M. A critical study of the Hopkinson pressure bar. *Philos. Trans. A* **240** (1948) pp. 375-457.
6. Follansbee, P. S. & Frantz, C. Wave Propagation in the Split Hopkinson Pressure Bar. *J. Engng. Mater. Tech.* **105** (1983) pp. 61-66.
7. Gong, J.C. Malvern, L.E. & Jenkins, D. A. Dispersion investigation in the split Hopkinson pressure bar. *J. Engng. Mater. Tech.* **112** (1990) pp. 309-314.
8. Gorham, D. A. A numerical method for the correction of dispersion in pressure bar signals. *J. Phys. E : Sci. Instrum.* **16** (1983) pp. 477-179.
9. Gorham, D. A. & Wu, X. J. An empirical method for correcting dispersion in pressure bar measurements of impact stress. *Meas. Sci. Technol.*, **7** (1996) pp. 1227-1233.
10. Hillström, L. Mossberg, M. & Lundberg, B. Identification of complex modulus from measured strains on an axially impacted bar using least squares. *J. Sound Vibration* **230** (2000) pp. 689-707.
11. Lundberg, B. & Blanc, R. H. Determination of mechanical material properties from the two-point response of an impacted linearly viscoelastic rod specimen. *J. Sound Vibration* **126** (1988) pp. 97-108.
12. Pochhammer, L. Über die Fortpflanzungsgeschwindigkeiten kleiner Schwingung in einem unbegrenzten isotropen Kreiscylinder. *J. für die Reine und Angewandte Mathematik* **81** (1876) pp. 324-336.
13. Othman, R., Blanc, R. H., Bussac, M. N., Collet, P. & Gary, G. A spectral method for wave dispersion analysis. Application to an aluminium rod. *Proceedings of the 4th International Symposium of Impact Engineering, Vol. I*, A. Chiba & S. Tanimura (2001) pp. 71-76.
14. Othman, R. R., Blanc, R. H., Bussac, M. N., Collet, P. & Gary, G. Identification de la relation de la dispersion dans les barres. *C. R. Acad. Sci. Série IIb* (2002) accepted for publication.
15. Zhao, H. & Gary, G. A three dimensional analytical solution on of the longitudinal wave propagation in an infinite linear viscoelastic cylindrical bar, application to experimental techniques. *J. Mech. Phys. Solids* **43** (1995) pp. 1335-1348.